LBL-13719

Lawrence Berkeley Laboratory
UNIVERSITY OF CALIFORNIA

Materials & Molecular
Research Division

EVIDENCE FOR BIFURCATION AND UNIVERSAL CHAOTIC BEHAVIOR IN NONLINEAR SEMICONDUCTING DEVICES

James Testa, José Pérez, and Carson Jeffries

January 1982

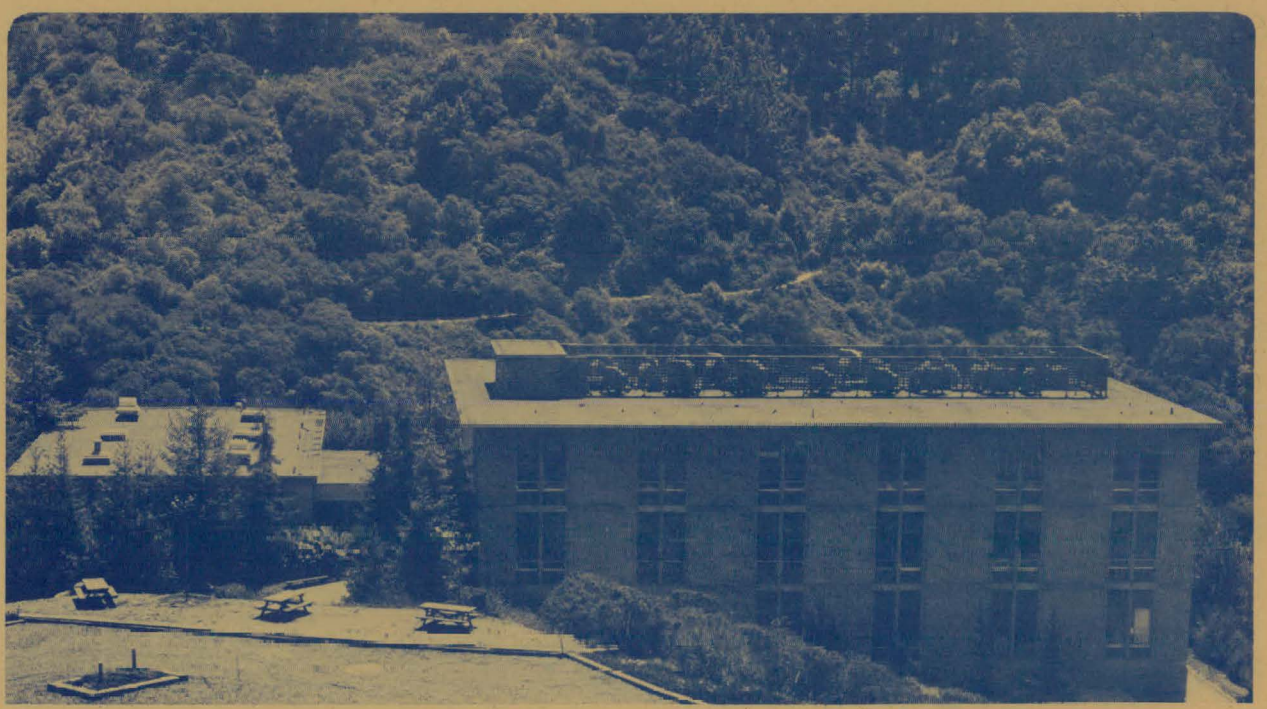

Prepared for the U.S. Department of Energy under Contract W-7405-ENG-48

DISCLAIMER

Printed in the United States of America
Available from
National Technical Information Service
U.S. Department of Commerce
5285 Port Royal Road
Springfield, VA 22161
Price Code: A03

LBL--13719

DE82 011106

EVIDENCE FOR BIFURCATION AND UNIVERSAL CHAOTIC BEHAVIOR IN NONLINEAR SEMICONDUCTING DEVICES*

James Testa, José Pérez, and Carson Jeffries

Materials and Molecular Research Division, Lawrence Berkeley Laboratory, and Department of Physics, University of California, Berkeley, CA 94720

ABSTRACT

Bifurcations, chaos, and extensive periodic windows in the chaotic regime are observed for a driven LRC circuit, the capacitive element being a nonlinear varactor diode. Measurements include power spectral analysis; real time amplitude data; phase portraits; and a bifurcation diagram, obtained by sampling methods. The effects of added external noise are studied. These data yield experimental determinations of several of the universal numbers predicted to characterize nonlinear systems having this route to chaos.

*This work was supported by the Director, Office of Energy Research, Office of Basic Energy Sciences, Material Sciences Division of the U. S. Department of Energy under Contract No. W-7405-ENG-48.

I. Introduction

There is at present a revival of interest in nonlinear dissipative systems, largely due to recent theoretical developments from topology and the computed behavior of simple recursion relations, or maps, e.g., the logistic difference equation $x_{n+1} = \lambda x_n(1-x_n)$.[1-3] This is perhaps the simplest nonlinear expression, and much more readily calculable than the nonlinear *differential* equations of most physical systems. As discussed in Section III, the logistic model predicts period doubling bifurcations; onset of chaos (noise); and periodic windows in the chaotic region. The behavior is quantitatively characterized by several "universal numbers", obtained by computer iteration. These are somewhat analogous to critical exponents in the theory of critical phenomena. The prediction and the hope is that the behavior of such simple maps will qualitatively and even semi-quantitatively explain the actual behavior of real systems. There are many examples of nonlinear behavior in condensed matter physics which give rise to instabilities and noise, not yet well understood. The objective of this report is to study in detail a driven nonlinear semiconducting oscillator, using several methods, and to compare its behavior with the logistic model. The data yield "measured values" for several of the universal numbers, some for the first time. The overall agreement is surprisingly good. Studies of similar physical systems are in progress; the tentative results are also understandable in terms of the logistic model. Feigenbaum[1] has shown that a large class of maps having a quadratic maximum exhibit the same universal behavior as the logistic map.

II. System

The nonlinear electrical oscillator used in this experiment was a LRC circuit as shown in Figure 1. A heavily doped silicon diode, type 1N953 manufactured by TRW Company, supplied the nonlinear capacitance.[4] The capacitance across the varactor varies with reverse applied voltage as

$$C(V) = \frac{C_o}{(1+V/b)^{\beta}} \tag{2.1}$$

where $C_o \approx 300$ pF, $b \approx 0.6$ volts, and $\beta \approx 0.5$. For the *reversed* half of a cycle when the diode is in the nonconducting capacitance state, the circuit driven by an oscillator obeys the equation

$$\frac{Ld^2Q}{dt^2} + \frac{RdQ}{dt} + (1 + \frac{V}{b})^{\beta} \frac{Q}{C_o} = V_o \sin(2\pi ft) \tag{2.2}$$

where the relation

$$V(Q) = (1 + \frac{V}{b})^{\beta} \frac{Q}{C_o} \tag{2.3}$$

can be used to eliminate V in the third term on the left. This yields a complicated nonlinear oscillator of form $L\ddot{Q} + R\dot{Q} + \frac{1}{C_o} f(Q) = V(t)$. In the *forward* (conducting) phase the function $f(Q)$ is different, the diode being chiefly conducting, with negligible capacitance. The objective of this paper is not to solve these intractable equations, but rather to take data on this physical system and compare it to the predictions of the simple logistic model. However, for the form $f(Q) = Q - 4Q^3$, the driven nonlinear oscillator problem has been solved by computer,[5] with solutions exhibiting behavior similar to the logistic model.

III. Theory

One of the paths a driven system can take that leads to chaotic, or turbulent, behavior is that of period doubling bifurcations, calculable, e.g. from the logistic recursion relation

$$x_{n+1} = \lambda x_n(1-x_n), \qquad (3.0)$$

where λ is the control parameter or driving force. For $0 < \lambda < 4$, x lies in the interval $0 < x < 1$; the resulting bifurcation diagram is shown in Figure 2. As λ is increased, there is a threshold value λ_1 where the iteration of Eq. 3.0 yields two values of x, and the power spectrum shows a new component at f/2. As the system is driven harder (λ further increased) more bifurcation thresholds (denoted by λ_n) and subharmonics appear at f/4, f/8, f/16, ..., $(f/2^n)$..., until $n \to \infty$, which is the threshold for the chaotic state at λ_c. At this point pseudo-random noise begins. For $\lambda > \lambda_c$, a sequence of inverse bifurcations or noise band mergings occurs, Figure 2, at M_n, n = ...3, 2, 1, 0, where 2^{n+1} bands merge to 2^n bands.[2] After the point where chaos (noise) occurs is reached, there appear windows (see Fig. 2) in this noisy region that are noiseless. These windows are periodic at subharmonic frequencies f/m, where m = 1, 2, 3, 4...; some show subsequent bifurcations within the window width. These new bifurcations lead to chaos (noise) again.

All of this behavior obeys certain universal properties irrespective of the exact details of the system. According to the latest developments of the theory of the bifurcations, there are a number of universal numbers that occur in a bifurcating system. The first one to be computed, by Feigenbaum,[1] is the convergence rate δ, which is defined as

$$\delta = \lim_{n \to \infty} \left[\frac{\lambda_{n+1} - \lambda_n}{\lambda_{n+2} - \lambda_{n+1}} = \delta_n \right] = 4.669... \qquad (3.1a)$$

where λ_n is the threshold value of the driving parameter for the system where the n^{th} bifurcation occurs, and $f_n = f/2^n$.

Feigenbaum also computed the number

$$\alpha = 2.5029... \qquad (3.1b)$$

which measures the ratio of the pitchfork separation in the upper and lower bifurcations, Figure 2.

The average height of the peaks of the odd subharmonics in a power spectral plot from one bifurcation to the next is predicted to be[6]

$$2\beta^{(2)} = 20.963... = \lim_{n \to \infty} \left[\frac{\frac{1}{2^{n-1}} \sum_{i}^{2^{n-1}} P[(2i+1)\, f_n]}{\frac{1}{2^n} \sum_{i}^{2^n} P[(2i+1)\, f_{n+1}]} \right] \qquad (3.2)$$

where f_n is the frequency of the n^{th} bifurcation and P[f] is the power of the subharmonic of frequency, f.

In the chaotic region the noise-free periodic windows are predicted to occur in a certain order[7] and at certain values of the driving parameter $\lambda_{K,q}$, according to[8]

$$\bar{\lambda}_K - \lambda_{K,q} = A\delta^{-K}\gamma_K^{-q} \qquad (3.3)$$

Here $\bar{\lambda}_K$ is the point where 2^K bands merge into 2^{K-1} bands in inverse bifurcation; $\lambda_{K,q}$ is the threshold point where the period q occurs between mergings $\bar{\lambda}_K$ and $\bar{\lambda}_{K-1}$, and A is a constant.

As $K \to \infty$, it has been computed[8] that γ_K approaches

$$\gamma = 2.948..., \qquad (3.3a)$$

which is another universal number.

The effect of added external noise on the system has been predicted to be governed by universal constants, also. Assume that one can observe periodic behavior of at most period $q \cdot 2^p$ at a noise level Λ_p. If the noise voltage level is reduced by a factor[9,12]

$$\kappa = 6.619... \qquad (3.4)$$

then one will be able to resolve an additional period $q \cdot 2^{p+1}$.

It is also predicted[10] that the rms spectral band width at the n^{th} bifurcation, W_n, obeys,

$$W_n = W_o \beta^{-n} \tag{3.5}$$

where

$$\beta = 3.2375... \tag{3.5a}$$

is another universal number.

The integrated noise power spectrum, $N(\lambda)$, also obeys a scaling relation,[10] given by

$$N(\lambda) = N_o(\lambda - \lambda_c)^{\sigma} \tag{3.6a}$$

where

$$\sigma = \frac{2 \ln \beta}{\ln \delta} = 1.5247..., \tag{3.6b}$$

The Lyapunov characteristic exponent $\bar{\lambda}$ (not to be confused with the control parameter λ) also obeys a scaling relation,[11]

$$\bar{\lambda} = \bar{\lambda}_o(\lambda - \lambda_c)^{\tau} \tag{3.7a}$$

where

$$\tau = 0.4498069... = \frac{\ln 2}{\ln \delta} \tag{3.7b}$$

And at λ_c, $\bar{\lambda}$ scales with added noise Λ as[9]

$$\bar{\lambda}(\lambda = \lambda_c, \Lambda) = A\Lambda^{\theta} \tag{3.8a}$$

where

$$\theta = 0.37 \pm 0.01, \; A = 0.58 \pm 0.01 \tag{3.8b}$$

To summarize this section, it is clear that a number of computed "universal numbers" exist which characterize the bifurcation route to chaos. The simplest logistic model of nonlinearity, Eq. 3.0, has been used to compute most of these; however, it appears that essentially the same numerical values are computed for any simple nonlinearity with approximately

a quadratic maximum. In the next section of this paper we give measured values of several of these numbers.

IV. Experimental Results

A. Methods

In the experimental arrangement, Figure 1, the sine wave oscillator at a frequency fixed near f_{res} = 93 kHz, and variable voltage $V_o \sin(2\pi ft)$ is filtered by a narrow band filter; a digital AC voltmeter reads the amplitude V_o to within 1 mV. The role of the control parameter λ is played by the voltage V_o. The developed voltage across the nonlinear capacitor, which corresponds to x in Eq. 3.0, is amplified by a buffer, whose output V_c is used in several ways:

1) To measure the power spectrum (see Figs. 3 and 4) with a spectrum analyzer having a dynamic range of 85 db and sensitivity of 300 nV. Spectral components f/2 to f/32 are well resolved. It would be possible to observe components 95 db below V_o at f; however, the intrinsic noise of the varactor diode initiates chaos after f/32.
2) To display I(t) and $V_o(t)$ along the y and x axes of an oscilloscope, respectively, generating a phase portrait (see Fig. 5), analogous to the elliptical orbit of a harmonic oscillator in phase space $\dot{x}$, x.
3) To generate on a dual beam oscilloscope a real time display $V_c(t)$ (see Fig. 6), which shows directly the bifurcated subharmonic periods and the patterns of visitation of the oscillator to its various states.[7]
4) To generate by a fast sampling procedure[13] the actual bifurcation diagram (see Fig. 7) of the system, analogous to the (computed)

diagram of Figure 2. This is the first report of the direct measurement of a bifurcation diagram; it is a powerful technique for analysis of nonlinear behavior, and shows all the features of Figure 2, including bifurcation thresholds, onset of chaos, band mergings, windows, and a veiled structure corresponding to regions of high probability density.[9] The Figures 7a-7f show successive close-ups (using electronic zoom) of the universal pitchfork structure, over a scale of 100.

5) To generate, by sampling noise in a very narrow band near f/2 but not at any discrete subharmonic up to f/100, a noise scan (see Fig. 8), which displays directly the onset of chaos at $V_o = V_{crit}$ (i.e. $\lambda = \lambda_c$), and the many noise-free windows in the chaotic region.

B. Data

A run consisted of slowly increasing V_o and recording the threshold values V_{on} for bifurcation to a frequency $f/2^n$. The indication of a bifurcation was taken to be the appearance of this subharmonic in the frequency spectrum, with a signal 10 db above the noise level. An alternate but less sensitive method was visual observation of a splitting in the phase portrait on the x-y oscilloscope. Table I lists events and the voltage V_o at which they occur, for a frequency f = 99 kHz: periodic bifurcations, chaos, and a number of clear noiseless windows were observed, as well as many noisy windows. Notable is a wide and stable window that begins at V_o = 3.081 volts with period 3, and then bifurcates to periods 6, 12, 24, and 48, finally becoming noisy at 3.844 volts. These windows have the

ordering and the visitation patterns approximately as predicted in Ref. 7, and will be discussed in another paper[13]; they are visible in the bifurcation diagram, Figure 7, and the window scan, Figure 8.

From the thresholds for the prechaotic periodic bifurcations, we calculate for the convergence number

$$\delta_1 = \frac{V_{04} - V_{02}}{V_{08} - V_{04}} = 4.257 \pm 0.1 \qquad (4.1)$$

$$\delta_2 = \frac{V_{08} - V_{04}}{V_{016} - V_{08}} = 4.275 \pm 0.1 \qquad (4.2)$$

From an expansion of the bifurcation diagram, Figure 9, we are able to directly measure the number α for the first time; this figure shows the ratio of the splitting in the upper and lower branches at period 16, just before bifurcation to 32. From six independent measurements we find

$$\alpha = 2.43 \pm 0.1 \qquad (4.3)$$

By adding external noise from a random noise generator to the sine wave excitation, it was possible to observe both from the power spectrum and the bifurcation diagram that increasing noise obliterates successively the bifurcations. In Table II the data are presented. From the voltage ratio required to obliterate successive bifurcations, we measure the average value

$$\kappa = 6.30 \qquad (4.4)$$

The number $2\beta^{(2)}$, Eq. 3.2, expressed as 10 log(20.963) = 13.21 db, can be experimentally determined by comparing the average of the peaks in the power spectra between two successive bifurcations. For our data where average peaks between 0 and f/2 are recorded, it is more convenient to

compare the individual peaks to the predictions of the logistic model, shown, e.g. in Ref. 2, page 53, and as dashed bars in Figure 3. The data show reasonable agreement with a rms deviation of ∿2 db.

By integrating the smoothed broad-band noise power $P(f)$, $N(\lambda) = \int_0^{f/2} P(f)df$ for spectral analysis data taken at successive band mergings M_n in the chaotic regime, we obtained a measured value of the number β, using the expression[10]:

$$N(M_{n+1}) = N(M_n)\beta^{-2} \tag{4.5}$$

For data taken at band mergings M_3, M_2, M_1, and M_0, corresponding to the merging to 8, 4, 2, and 1 bands, respectively (see Figs. 7a, 7c, and 7e), we find the average value

$$\beta = 3.26 \pm 0.9 \tag{4.6}$$

V. Summary

Table III collects the principal results of this paper, the measured values of universal numbers for the real physical system, Fig. 1, and compares them to the values predicted by the logistic model. Considering that the actual nonlinear differential equations, Eqs. 2.2 and 2.3, of the anharmonic oscillator are much more complex than the simple logistic nonlinear expression, Eq. 3.0, it is concluded that the agreement is surprisingly good. These are the first direct experimental measurements [as contrasted to computed (numerical) experiments] for α, κ, and β. The strong similarity between the observed and predicted bifurcation diagram gives further support to the utility of simple models as a key to chaotic behavior of nonlinear systems. The measurement of the bifurcation diagram is a powerful method for assessing the degree to which this route, or other routes,[14] a particular physical system will follow. For example, Figure 10 shows the bifurcation diagram observed for a circuit like Figure 1, but with

a higher driving oscillator impedance: the diagrams differ ar large values of V_0; the bifurcation diagram is quite sensitive to small changes in system parameters.

We wish to thank Joseph Rudnick, Michael Nauenberg, Jim Crutchfield, M. P. Klein, and Howard Shugart for helpful conversations. This work was supported by the Director, Office of Energy Research, Office of Basic Energy Sciences, Material Sciences Division of the U. S. Department of Energy under Contract number W-7405-ENG-48.

References

[1]M. J. Feigenbaum, Los Alamos Science 1, 4 (1980); J. Stat. Phys. 19, 25 (1979).

[2]For a review, see P. Collet and J.-P. Eckmann, Iterated Maps on the Interval as Dynamical Systems (Birkhauser Press, Boston 1980).

[3]For an earlier preview, see R. M. May, Nature 261, 459 (1976), with implications for biological and socio-economic systems.

[4]A varactor as a nonlinear element in bifurcation experiments was first reported by P. Linsay, Phys. Rev. Lett. 47, 1349 (1981); for a discussion of varactors see B. G. Streetman, Solid State Electronic Devices (Prentice-Hall, 1972), p. 216.

[5]B. A. Huberman and J. P. Crutchfield, Phys. Rev. Lett. 43, 1743 (1979).

[6]M. Nauenberg and J. Rudnick, Phys. Rev. B24, 493 (1981).

[7]N. Metropolis, M. L. Stein, and P. R. Stein, J. Comb. Theory 15A, 25 (1973).

[8]T. Geisel and J. Nierwetberg, Phys. Rev. Lett. 47, 975 (1981).

[9]J. P. Crutchfield, J. D. Farmer, and B. A. Huberman, preprint, to be published in Reports in Physics.

[10]B. A. Huberman and A. B. Zisook, Phys. Rev. Lett. 46, 626 (1981).

[11]B. A. Huberman and J. Rudnick, Phys. Rev. Lett. 45, 154 (1980).

[12]J. Crutchfield, M. Nauenberg, and J. Rudnick, Phys. Rev. Lett. 46, 933 (1981).

[13]Carson Jeffries, José Pérez, and James Testa, to be published.

[14]J.-P. Eckmann, Rev. Mod. Phys. 53, 643 (1981).

Table I

Period	Threshold V_o rms volts	Comments
2	0.639	
4	1.567	
8	1.785	Threshold for periodic bifurcation
16	1.836	
32	1.853	
chaos	1.856	Onset of noise
12	1.901	
24	1.9012	Clear window with bifurcation
	1.905	
16	1.936	Noisy window
14	1.996	Noisy window
10	2.024	Noisy window
6	2.073	
12	2.074	Clear window with bifurcation
	2.077	
5	2.353	
10	2.363	Clear window with bifurcation
	2.371	
9	2.506	Noisy window
7	2.693	
14	2.096	Clear window with bifurcation
	2.700	
3	3.081	
6	3.538	
12	3.711	Clear wide window with extensive bifurcation
24	3.821	
48	3.841	
	3.844	
18	3.913	Noisy window
15	4.056	Noisy window
9	4.145	
18	4.154	Clear window with bifurcation
	4.158	
3	4.316	Noisy window
13	5.232	Clear window with bifurcation
26	5.246	
8	6.292	Window with flicker noise

Table II

Periods Observable	Noise Voltage (mV rms)
16, 8, 4, 2, 1	0.2 (initially present)
8, 4, 2, 1	10 ± 2
4, 2, 1	60 ± 5
2, 1	400 ± 25
1	2500 ± 500

Table III

Universal Number		Computed Value	Measured Value	(This work)
δ	(Eq. 3.1a)	4.669...	4.26 ± 0.1	(Eqs. 4.1, 4.2)
α	(Eq. 3.1b)	2.502...	2.43 ± 0.1	(Eq. 4.3)
$2\beta^{(2)}$	(Eq. 3.2)	13.2 db	11 to 15 db	(Fig. 3)
κ	(Eq. 3.4)	6.619...	6.29 ± 0.3	(Eq. 4.4)
β	(Eq. 3.5a)	3.237...	3.26 ± 0.9	(Eq. 4.6)

Figure Captions

Fig. 1 Schematic diagram of apparatus (XBL 821-7684).

Fig. 2 Computed bifurcation diagram $\{x_n\}$ vs λ, adapted from Ref. 9, showing bifurcation thresholds λ_1, λ_2...; chaos threshold λ_c; band mergings M1, M0; and windows of period 6, 5, and 3 (XBL 821-7677).

Fig. 3 Power spectral density (db) vs frequency, from zero to f/2 = 49 kHz in the prechaotic regime, showing subharmonic components f/2...f/32 with a dynamic range of 70 db. The intensities agree with prediction, dashed bars (Ref. 2), within an rms deviation ≈ 2 db (XBL 821-7683).

Fig. 4 Power spectral density (db) of bifurcated subharmonic components in the f/3 window in the chaotic regime (XBL 821-7685).

Fig. 5 The series circuit current I(t) (vertical axis) vs the varactor voltage $V_c(t)$ (horizontal axis); these phase portraits are shown for a series of values of the control parameter V_0 (see Table I). (a) Period f before first bifurcation. (b) Period 2 after bifurcation. (c) Period 4. (d) Period 16, expanded view. (e) Clear period 12 window in chaotic regime. (f) Clear period 5 window. (g) Clear period 3 window. (h) Merge M_1 into two bands. (i) Merge M_0 into one band. (XBL 821-7686)

Fig. 6 (a) Varactor voltage $V_c(t)$ and the sinusoidal "clock" voltage $V_0(t)$ for period 6 window at 2.073 V; the observed visitation pattern of the oscillator to its states is RLRRR, in agreement with Ref. 7. (b) A similar real-time signal for a bifurcated period 6 window at 3.538 V, with a

different pattern, RLLRL. The R signals, corresponding to the varactor reversed bias voltage, have clearly distinct values. The L signals occur in forward bias when the varactor diode is highly conducting, so that the voltage is highly compressed into the zero line (XBL 821-7682).

Fig. 7 (a) Measured bifurcation diagram, obtained by a scanning window comparator whose output V_y measures all the peak values of the varactor voltage V_c; this is done simultaneously with a much slower sweep (100 sec) of the driving oscillator voltage V_0 from 0 to 10 volts. The overall result has a close correspondence with Fig. 2, and various common points are identified ($\lambda_1 \rightarrow V_1$, etc.). Clear windows at periods 5, 7, 3, 6, 12, and 9 are identifiable. Only the upper half of Fig. 2 is recorded for reasons discussed in Fig. 6 (XBL 821-7678).
(b) Expansion of the bifurcation diagram of Fig. 7(a) (XBL 821-7687).
(c) Bifurcation diagram further expanded showing more clearly bifurcation thresholds V_3 (period 8) and V_4 (period 16); window of period 12; band merge M_1; and period 6 window (XBL 821-7679).
(d) Further expansion of the top half of Fig. 7(c) (XBL 821-7688).
(e) Further expansion of the lower half of Fig. 7(c) (XBL 821-7689).
(f) Further expansion of the bifurcation diagram, Fig. 7(c); the universal metric pitchfork scaling by $\alpha \approx 2.5$ is becoming evident (see Fig. 9) (XBL 821-7690).

Fig. 8 The noise power (in db) in a 300 Hz band width just below f/2 but resolved from it, vs the driving voltage V_0 (in peak volts), showing the

onset of noise (i.e. the onset of chaos); its rapid rise; and dips at windows of period 12, 6, 5, 7, 3, and 9. There is a hysteresis in the threshold for the period 3 window (XBL 821-7691).

Fig. 9 (a) The universal pitchfork structure, scaled by $\alpha = 2.502...$ as computed by Feigenbaum (Ref. 1). (b) The measured values of V_c (from an expanded bifurcation diagram) for the apparatus of Fig. 1, at period 16, just before the threshold for period 32. From the measured spacing we find $\alpha = a/b = 2.35$, and $\alpha = c/a = 2.61$.

Fig. 10 Bifurcation diagram for a system similar to that of Fig. 1, but with a larger driving source impedance. This diagram resembles Fig. 7(a) but differs at large values of V_0 (XBL 821-7692).

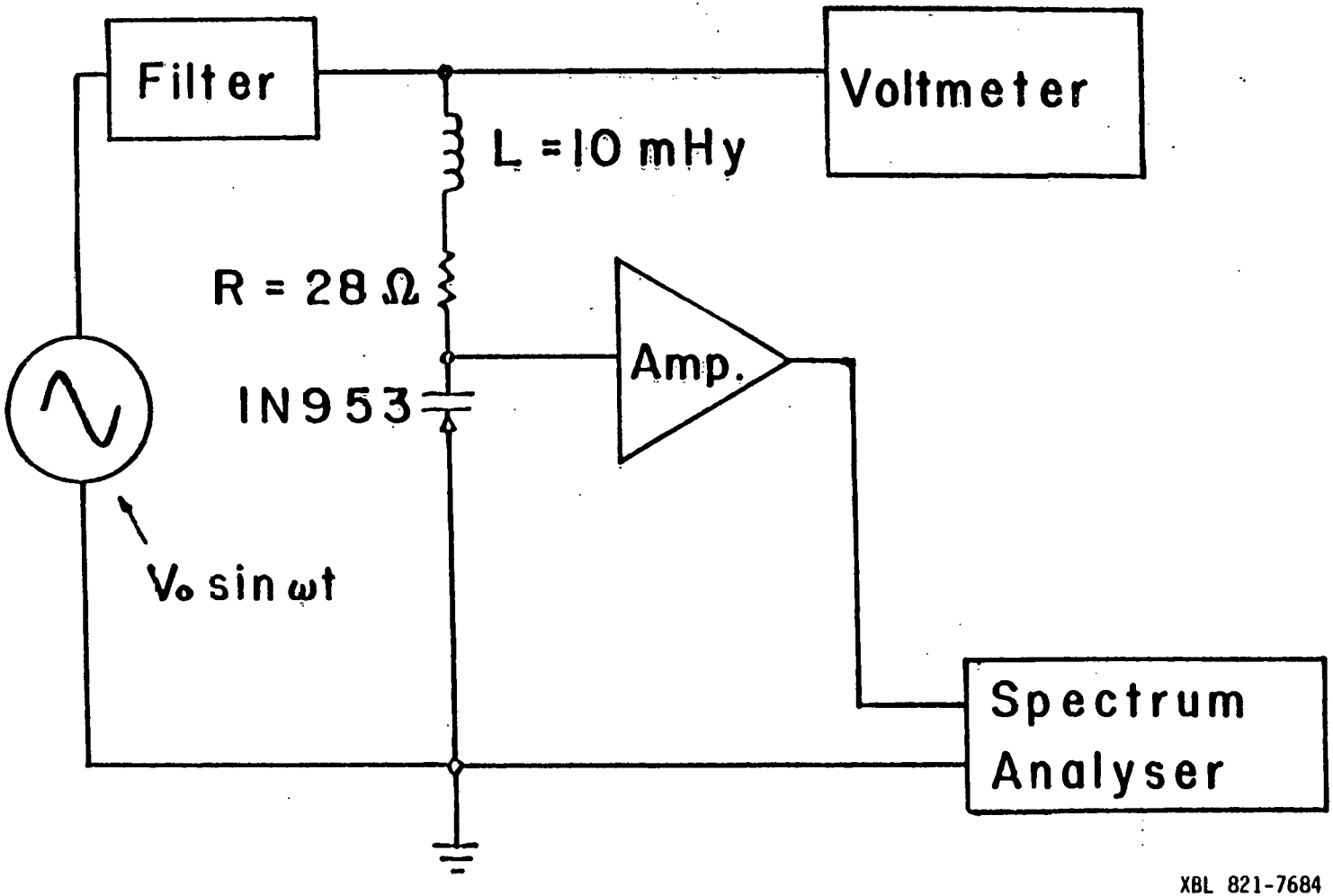
Filter
Voltmeter
L = 10 mHy
R = 28 Ω
Amp.
IN953
$V_o \sin \omega t$
Spectrum
Analyser
XBL 821-7684

FIG. 1

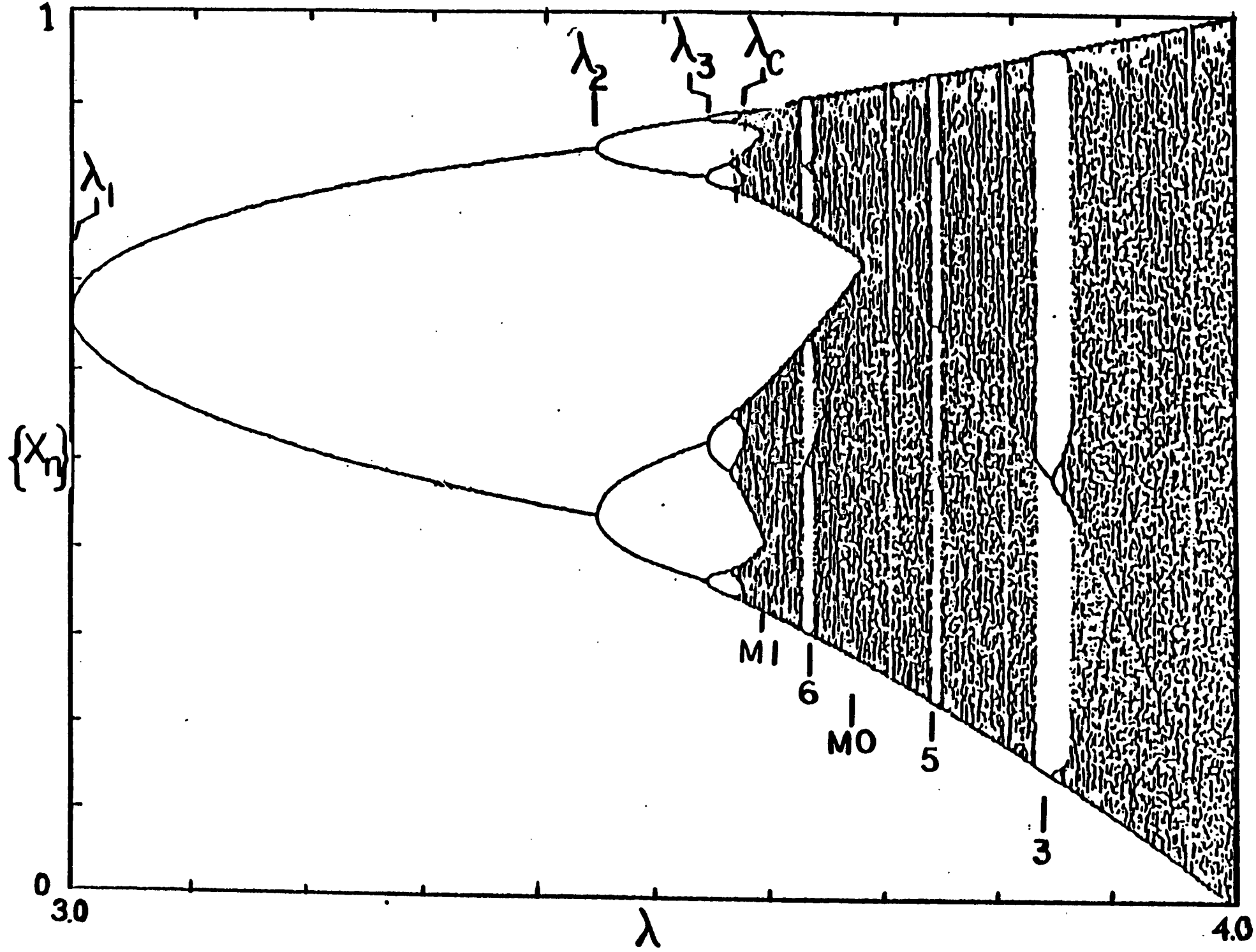

XBL 821-7677

FIG. 2

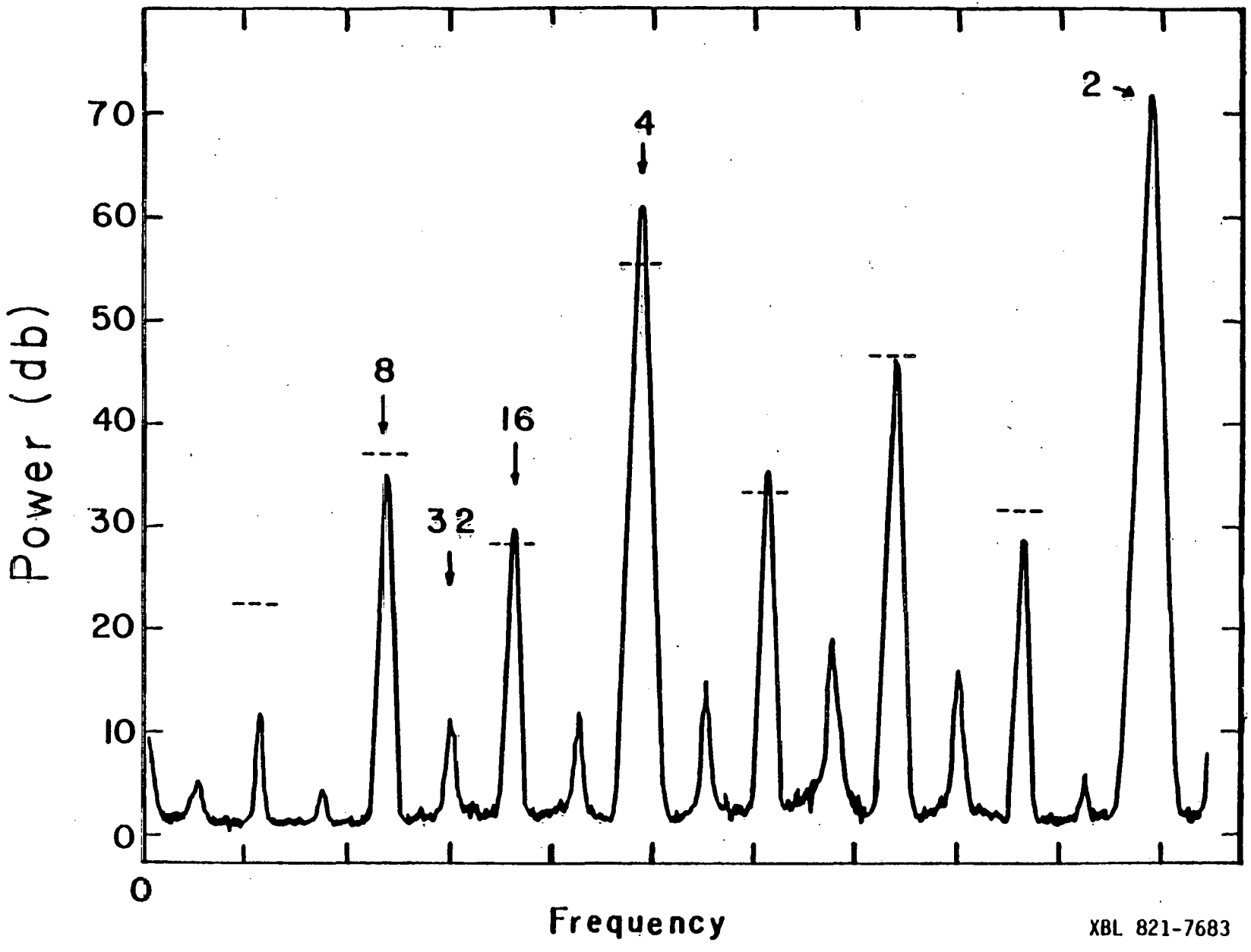

FIG. 3

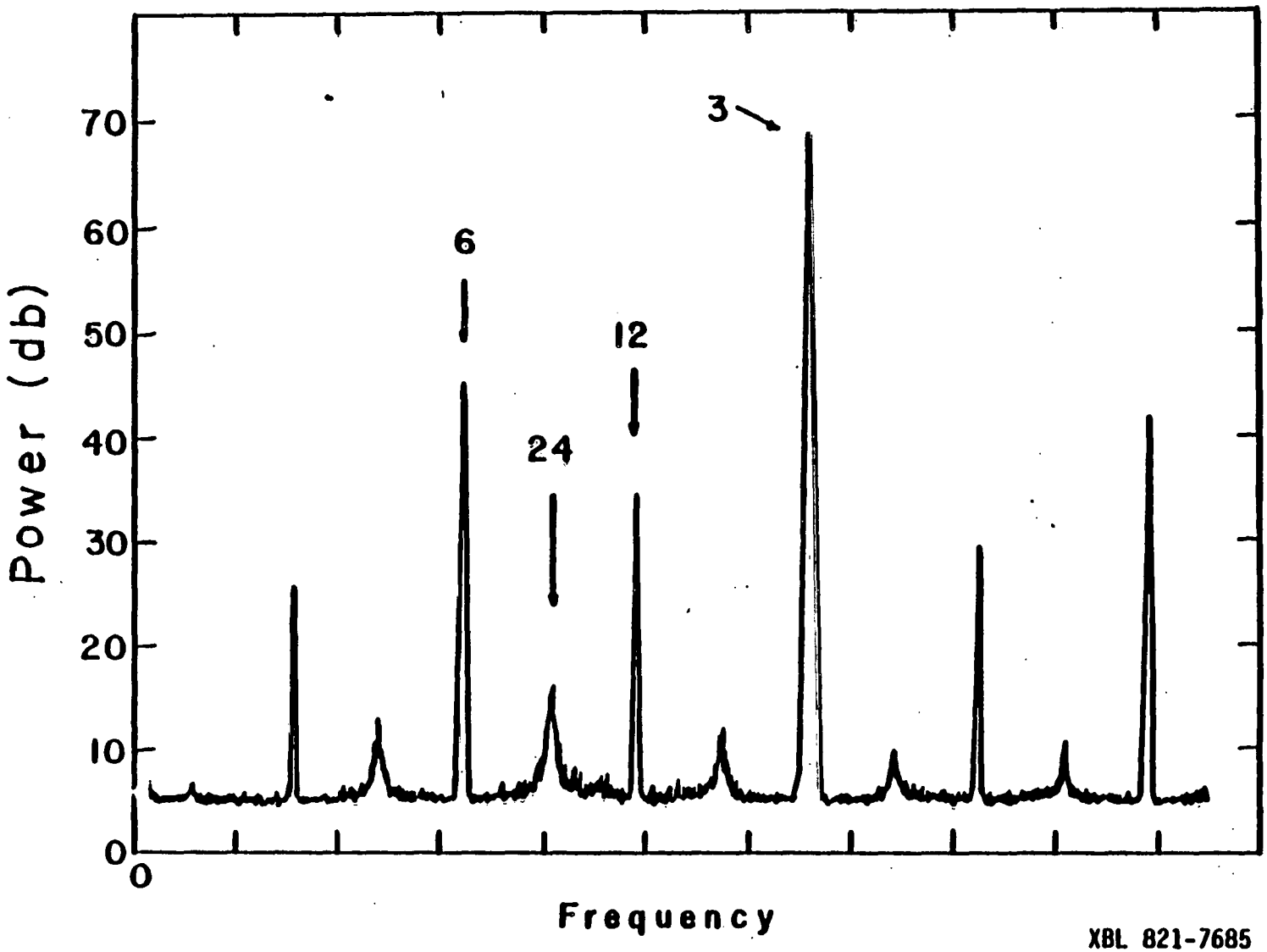

XBL 821-7685

FIG. 4

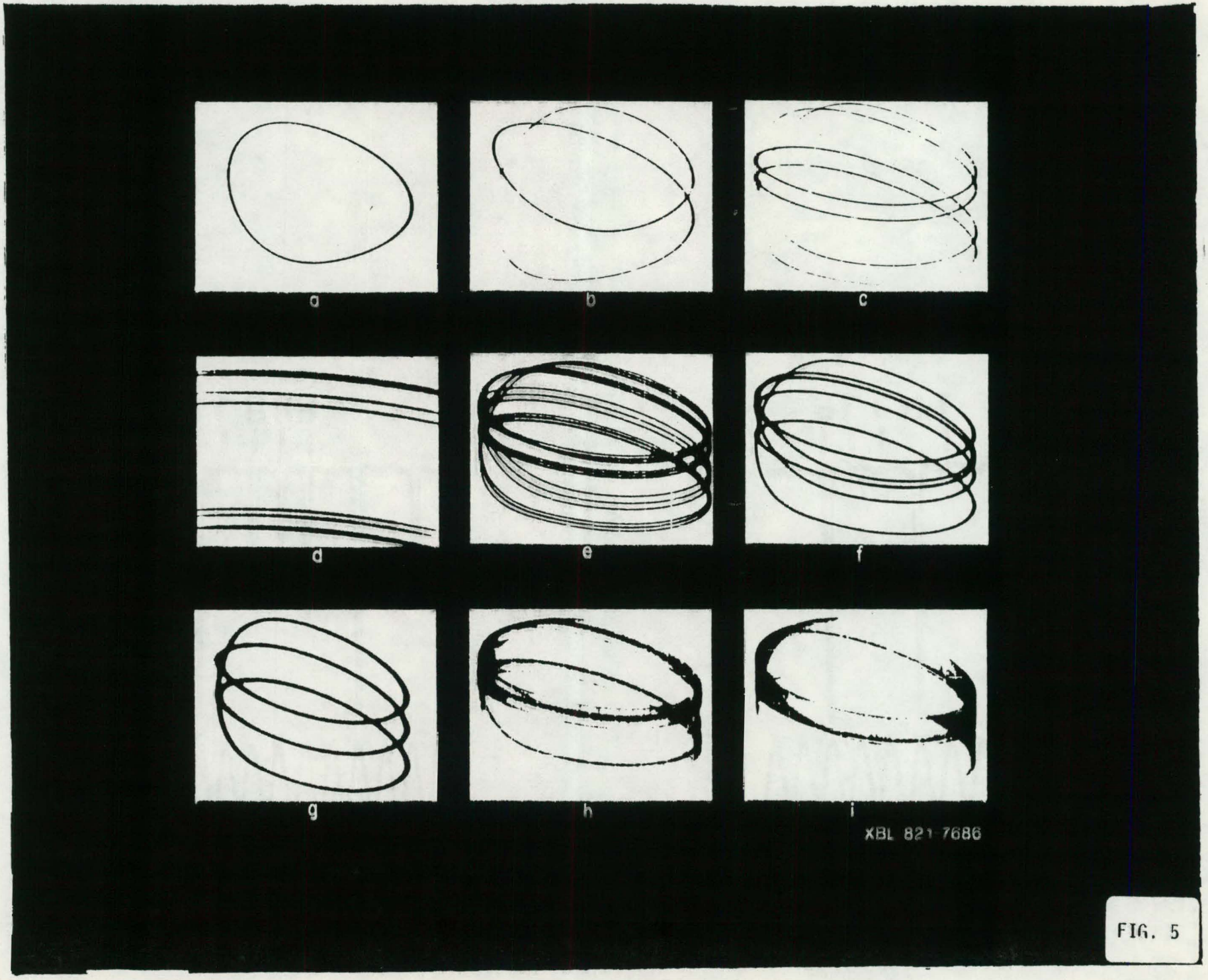

FIG. 5

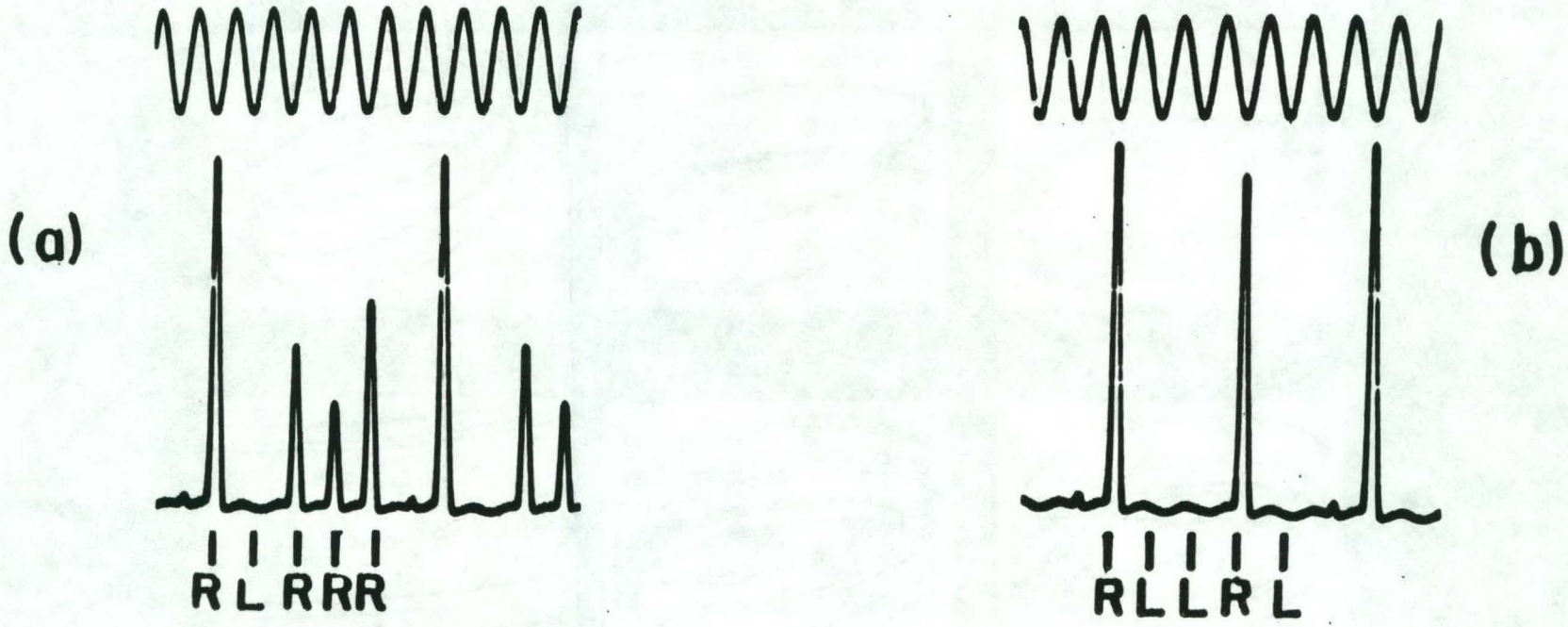

XBL 821-7682

FIG. 6

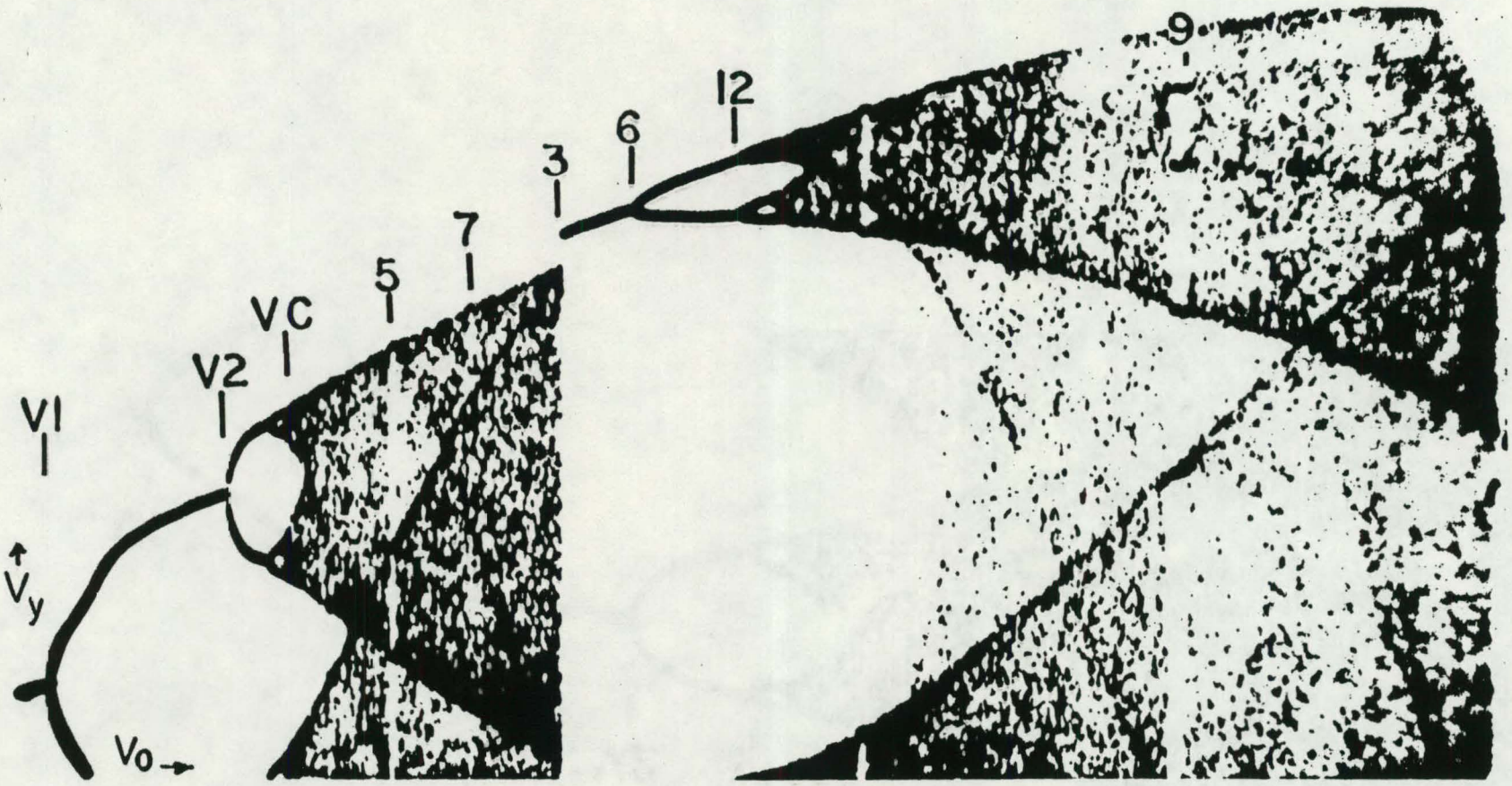

XBL 821-7678

FIG. 7a

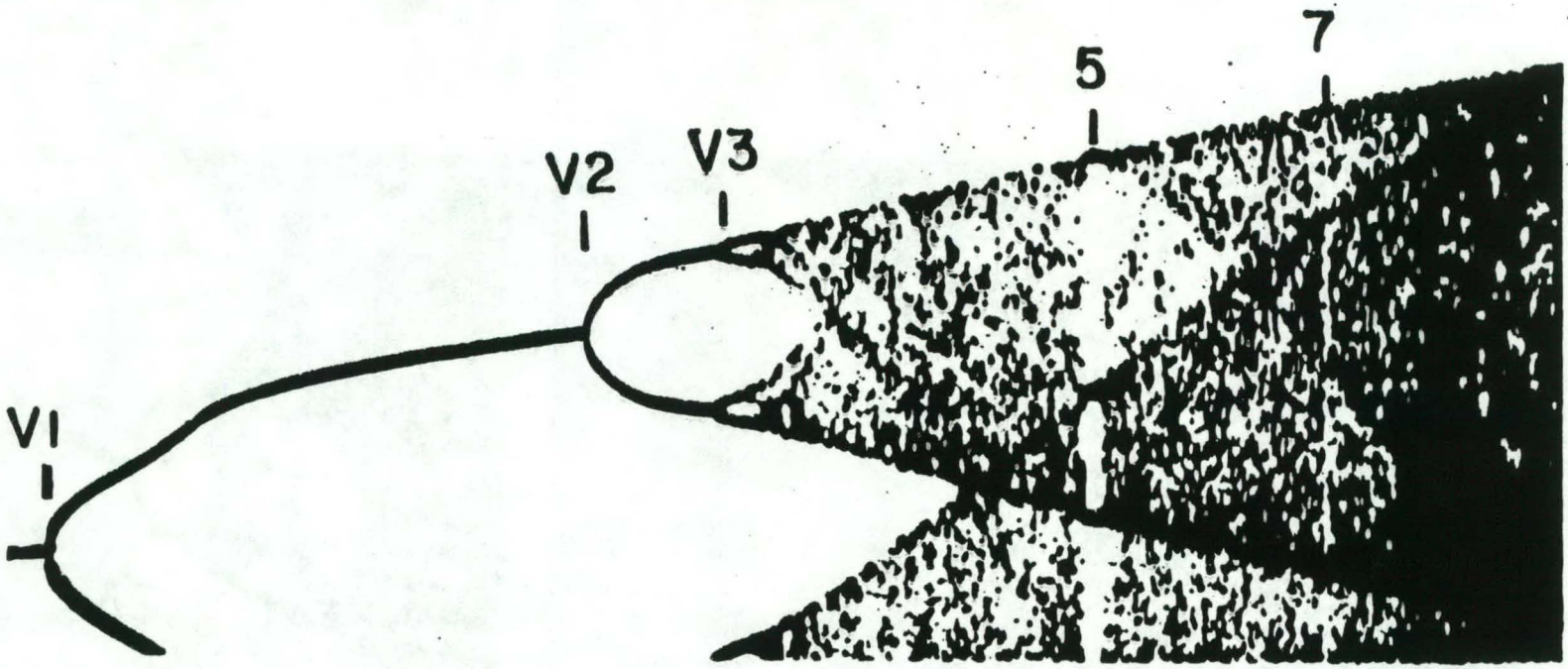

XBL 821-7687

FIG. 7b

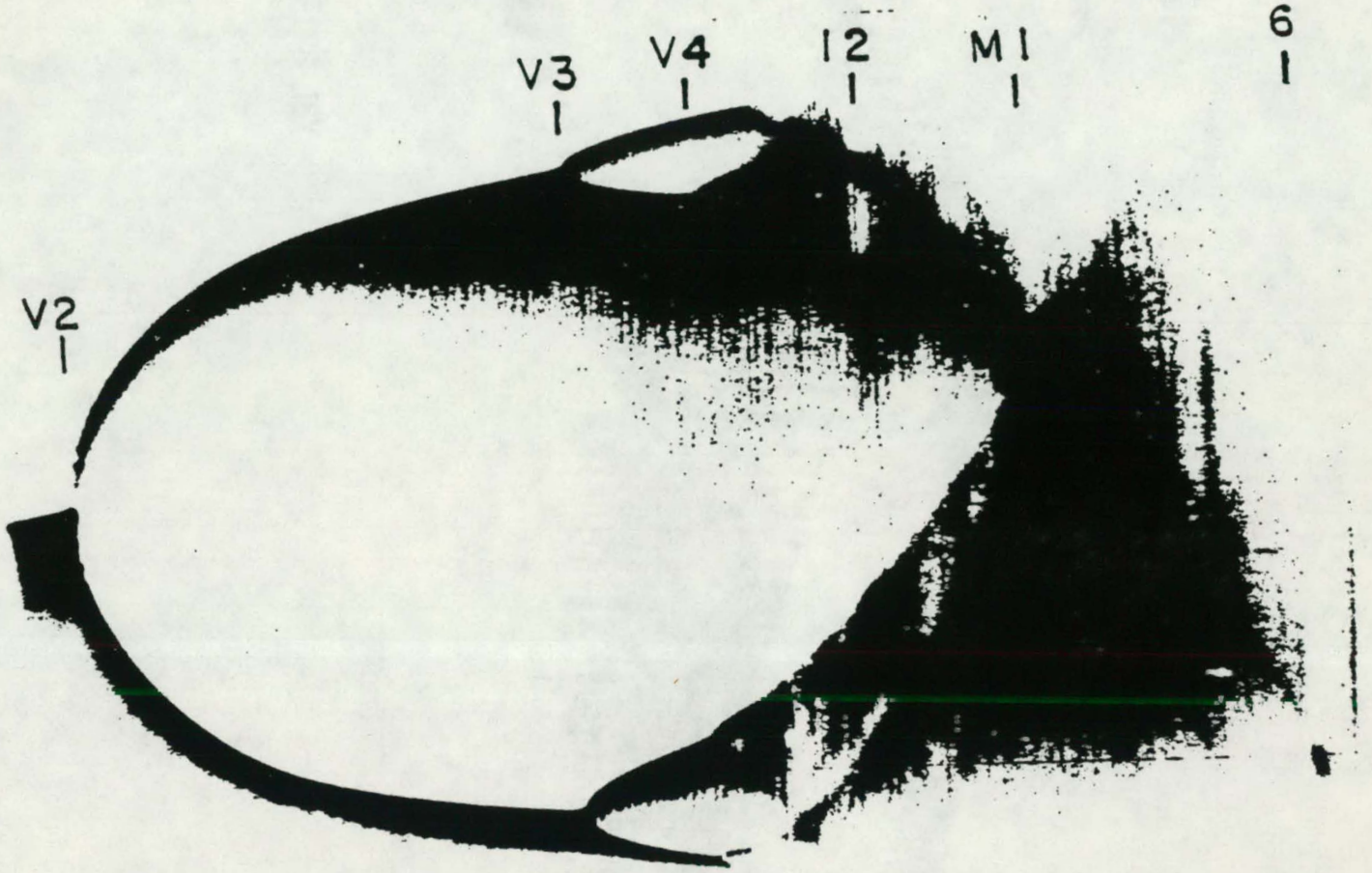

XBL 821-7679

FIG. 7c

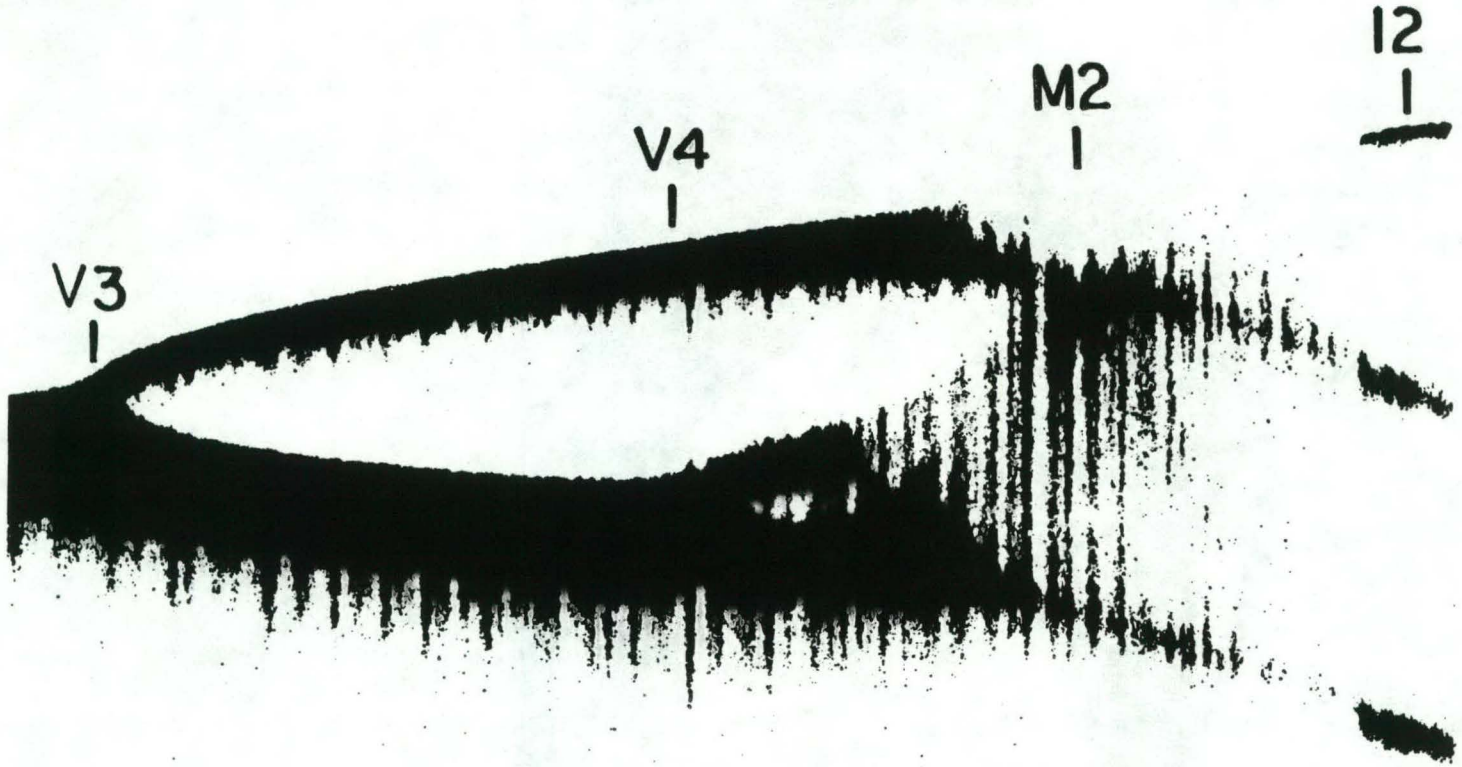

XBL 821-7688

FIG.7d

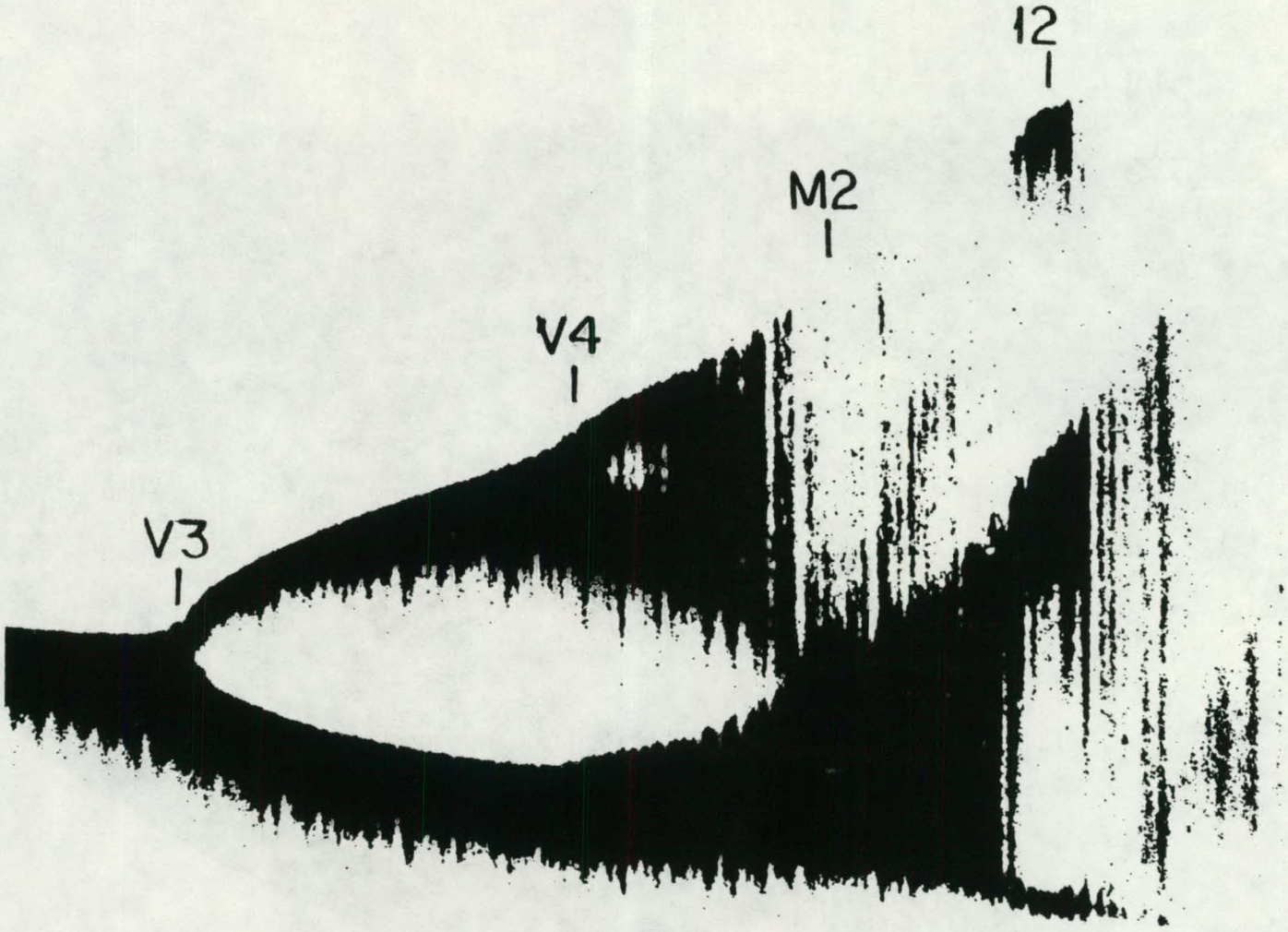

XBL 821-7689

FIG. 7e

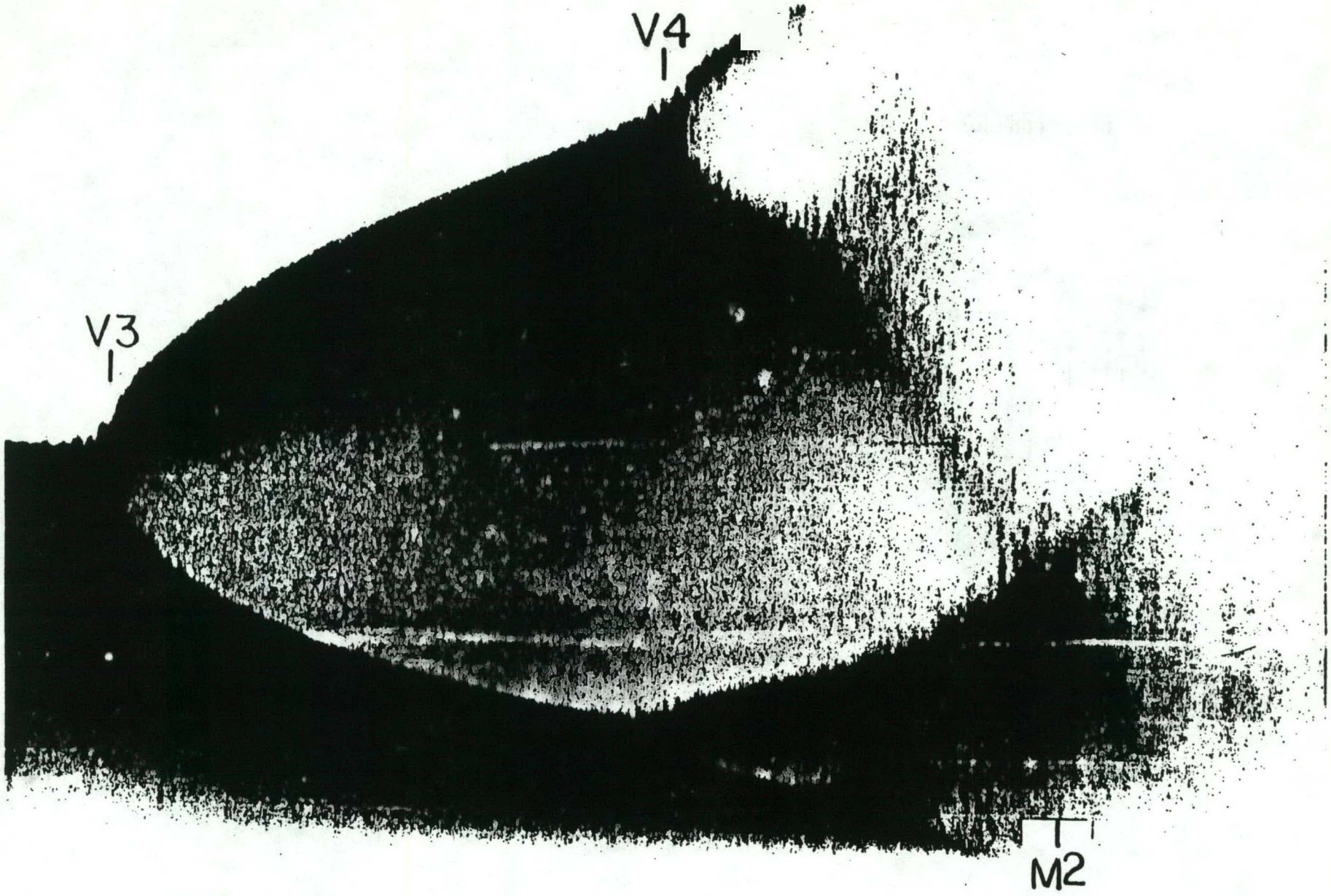

FIG. 7f

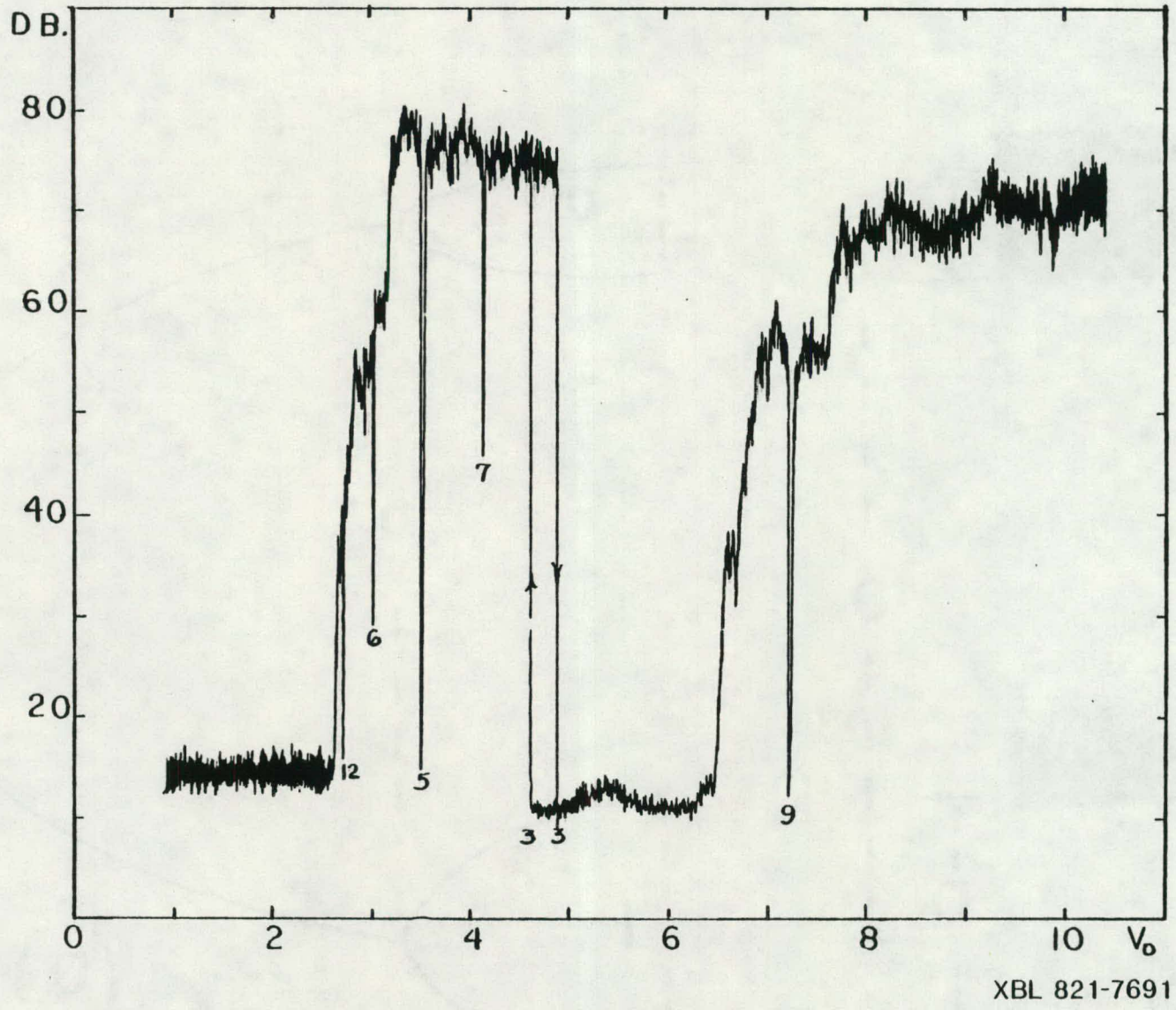

FIG. 8

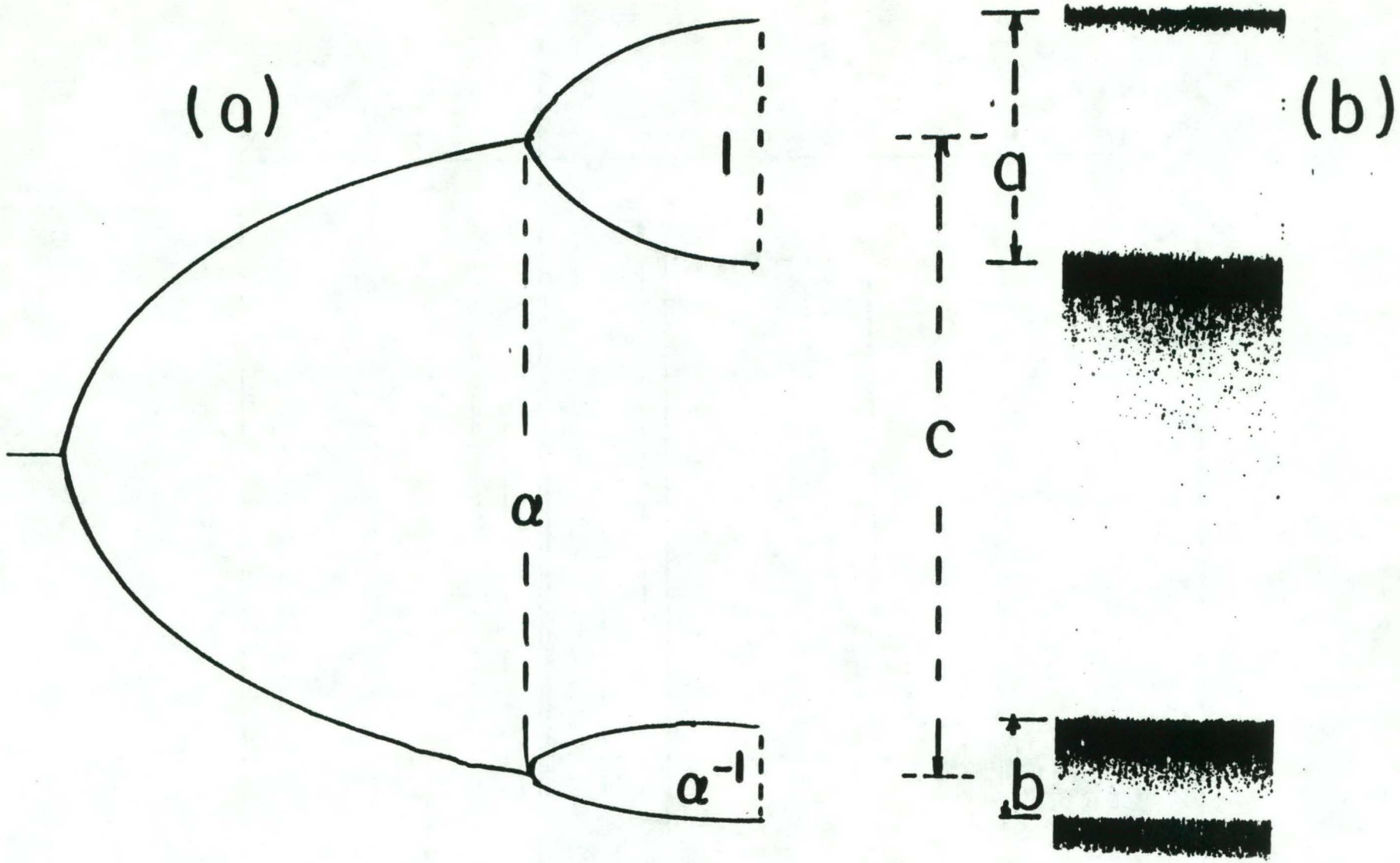

XBL 821-7681 FIG. 9

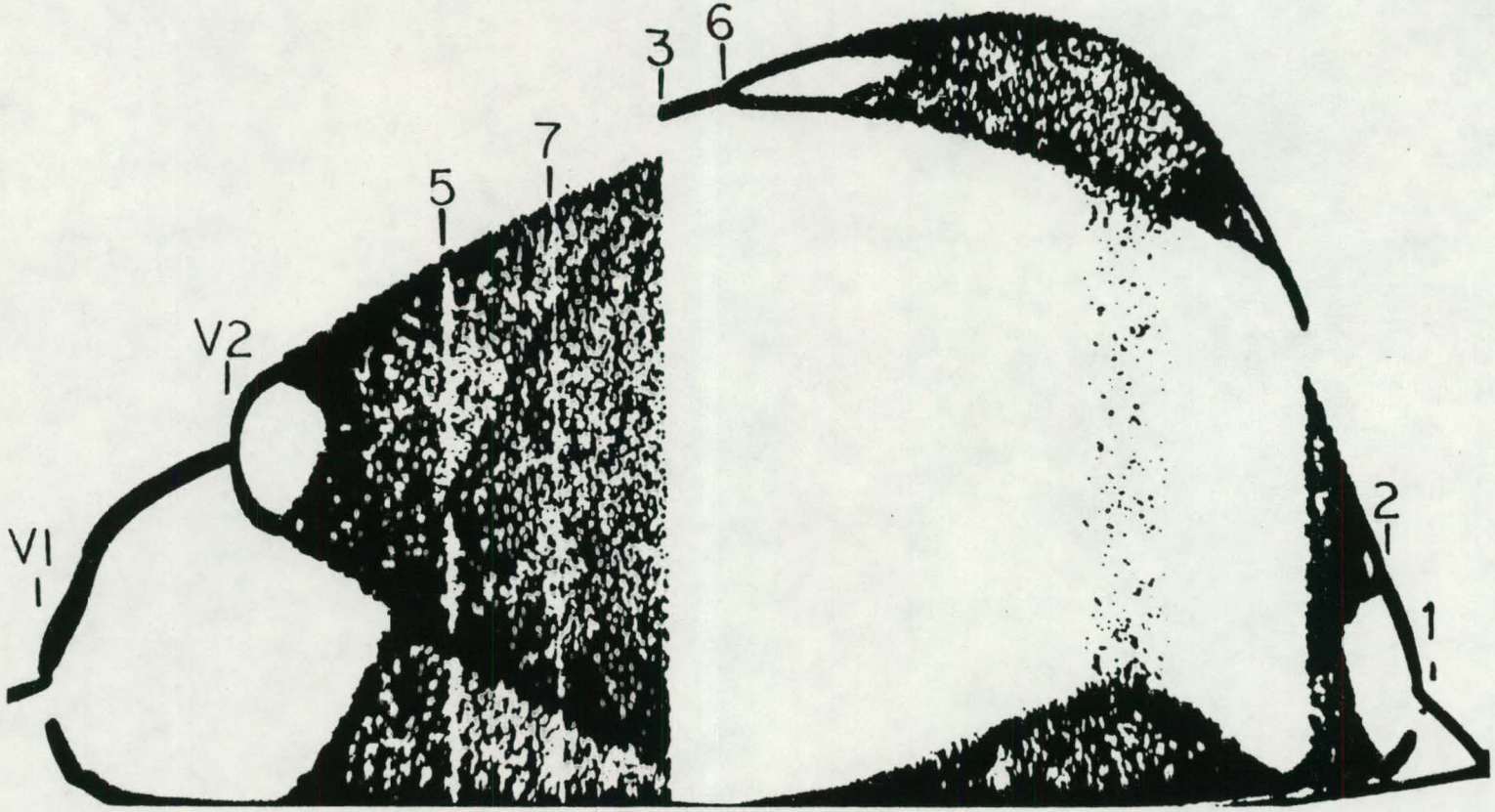

XBL 821-7692

FIG. 10

This report was done with support from the Department of Energy. Any conclusions or opinions expressed in this report represent solely those of the author(s) and not necessarily those of The Regents of the University of California, the Lawrence Berkeley Laboratory or the Department of Energy.

Reference to a company or product name does not imply approval or recommendation of the product by the University of California or the U.S. Department of Energy to the exclusion of others that may be suitable.

TECHNICAL INFORMATION DEPARTMENT
LAWRENCE BERKELEY LABORATORY
UNIVERSITY OF CALIFORNIA
BERKELEY, CALIFORNIA 94720